DIELECTRIC POLARIZATION

Dielectric materials have two major uses in electrical engineering: to insulate electrical components from one another (e.g., in cables and the mounting boards for electronic components, such as switch gear and active or inactive electronic devices) and to enhance the charge storage of capacitors. When in use as an insulator the major requirement is that no significant current should flow between the components, that is, the electrical impedance should be high. In the second case, under alternating current conditions, a capacitor is a more active element in that a current flows through a perfect insulator but is out of phase with the ac driving voltage applied to the plates. As a consequence, no power is dissipated as it is in a resistor in which current and voltage are in phase.

The term dielectric is due, as is much of our basic understanding of electrical phenomena, to Michael Faraday (1) and is an indicator that these materials support two different charge types, one positive and the other negative, when acted on by an electric field. Faraday, working in the early nineteenth century, came to this description by carrying out an experiment that is not difficult to repeat. The basic capacitor consists of two flat metal plates isolated from each other and mounted so that the planes of the plates are parallel and a small distance apart. The plates can be electrically charged by applying a voltage across them, and the amount of charge on each plate, Q, can be measured by disconnecting the voltage source and connecting the plates together so as to discharge the capacitor. Under the short-circuit condition, the current that flows from one plate of the capacitor to the other through the external connection can be measured as a function of time and integrated to give the original plate charge. Faraday observed, on applying a fixed voltage to the capacitor and comparing the charges on the plates when air filled the gap between them and when a dielectric material was inserted into this gap, that the quantity of stored charge increased and the amount by which it increased depended on the particular insulator inserted between the plates.

Writing the capacitance of the air-filled capacitor as C_0 we have, by experiment, that the capacitance in farads is given as

$$C_0 = Q/V = \epsilon_0 A/d \tag{1}$$

where (Fig. 1), A is the area of each plate and d is the separation between them, both in metric units, V is the applied voltage in volts, Q is the total charge on each plate (in coulombs), and ϵ_0, the permittivity of free space, is a constant and of magnitude 8.854×10^{-12} F · m^{-1}. On inserting the dielectric slab, which fills the space completely (Fig. 2), the new capacitance C_r can be expressed as a multiplicative factor of the original value:

$$C_r = \epsilon_0 \epsilon_r A/d \tag{2a}$$

$$= C_0 \epsilon_r \tag{2b}$$

where ϵ_r is the relative permittivity of the dielectric.

In this notation the relative permittivity of the empty space between the plates of the original air capacitor is taken as 1 and that of real dielectric insulators varies from about 2

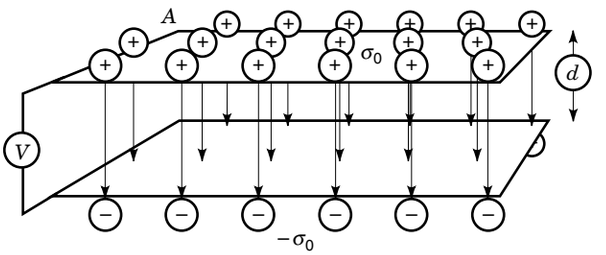

Figure 1. The voltage source of magnitude V is attached to two parallel plates, each of area A and separated by a distance d. With an air gap between the plates the voltage induces a surface charge of density σ_0, on each plate. The electric field in the gap, E_0, is given by $E_0 = V/d = \sigma_0 \epsilon_0$, where ϵ_0 is the permittivity of free space. The total charge on each plate is $Q = \sigma_0 \cdot A$, neglecting edge effects.

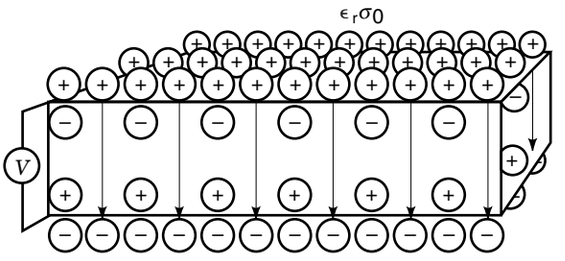

Figure 2. After a slab of dielectric of relative permittivity ϵ_r has filled the volume between the plates the charge on the surface of each plate increases in order to oppose the polarization of the dielectric until the *excess* charge at each plate returns to the original value of σ_0 and the *total* charge density on each plate is of magnitude $\sigma_0\epsilon_r$.

for polymers, to 80 for water. Table 1 presents a short list of materials and their relative permittivities and shows that groups of similar materials, in general, have similar values for their permittivity. For example, polymers, which are based on hydrocarbon chains, commonly have relative permittivities that are low; ionically bonded crystalline solids exhibit values of 4 to 10; covalently bonded semiconductors have permittivities in the range 16 to 20, and hydrogen-bonded water, whether as liquid or solid ice, has the large value quoted above.

The observation that the insertion of the dielectric gives an increased capacitive charge on the metal electrode plates for an unchanged applied voltage requires that the electric field between the plates, defined as the voltage per unit distance,

$$E = V/d \tag{3}$$

remains constant independent of the presence or absence of a dielectric. However, it is observed that on the insertion of the dielectric, charges flow from the voltage source to the plates. This can only occur if the insertion of the dielectric has led to a partial annulment of the original plate charges, which, in order to recover the initial equilibrium is required to be replaced from the potential source. The annulment arises from polarization within the dielectric, which gives rise to surface charges within the dielectric, which oppose the applied field as indicated in Fig. 2. We note from these figures that we require two sets of charges, one at each surface of the dielectric, and that these are of opposing sign; hence Faraday's choice of the term *di-electric* to describe materials that sustain charge separation under the action of an electric field.

Table 1. Permittivity Values

Material	Relative Permittivity	Material	Relative Permittivity
NaCl	6.0	Polyethylene	2.3
LiF	9.0	Polypropylene	2.2
Optical glass	6.0	Polystyrene	2.6
Mica	7.0	Polycarbonate	3.1
Quartz	4.5	PMMA	3.4/2.6
Diamond	5.7	Urea resin	5
Paraffin wax	2.2	Epoxy resin	3.5
Paraffin oil	2.2	Methanol	32.6
Castor oil	4.5	Ethanol	24.3
Transformer oil	2.2	Butanol	17.1
Water or ice	80	Liquid argon	1.53
Silicon	12	Liquid hydrogen	1.22
Germanium	16.3	Liquid oxygen	1.50

Now Table 1 begins to make sense. The proportion of plate charge that can be annihilated by a dielectric is a property of that particular dielectric. The general observation that polymers have low permittivities and semiconductors higher values tells us that it is the intrinsic structure and, in particular, the bonding within that structure that is important. The equivalence, in this context, of the permittivities of water and ice requires that the permittivity can be insensitive to the physical state of a material and must be based on local, molecular effects. In the particular case of water, although the magnitude of the response does not change in passing through the freezing or melting point, the rate at which water responds to an applied voltage, the relaxation time of the response, is some three or four orders of magnitude faster in the liquid than in the solid.

This simple analysis gives us sufficient information to define a dielectric. It is a material that responds to an electric field by forming, within the material at the surfaces directly adjacent to the electrodes, layers of positive and negative charges. The external driving potential responds by supplying additional charges until the voltage on the plates and hence the internal electric field maintain those of the air-filled cell. After the recovery the dielectric is fully polarized and can supply no further surface charge at that field. The magnitude of the equilibrium polarization, P, for the dielectric is then proportional to the applied field with

$$P = \epsilon_r\epsilon_0 E \tag{4}$$

Polarization is a bulk property, that is, it is uniform on any measure so we can reduce the size of the polarized entity down to atomic dimensions, at which point we take the smallest polarized particle to be a single dipole. A dipole is an entity with separated positive and negative charges and a polarization vector that is defined by the orientation of these charges to each other and of equivalent magnitude to that of the individual charges. In the simple parallel-plate capacitor, for example, we can consider that after insertion of the dielectric all the internal dipoles become aligned by the applied field. At any finite volume within the bulk of the dielectric the positive and negative charges cancel out and the only observable effect is the sheet of unbalanced positive charges of the surface layer of dipoles at the negatively charged electrode and the equivalent sheet of negative charges at the positive electrode.

There are, therefore, two areas of response. The first is the equilibrium situation, in which the driving potential has been applied for some time and the system is in equilibrium, which is termed electrostatics. The second is the response of the dielectric to a time-dependent voltage, typically either a step change in magnitude or a steady sinusoidal potential of frequency ω, the *ac* response or dispersion of the dielectric.

Electrostatics

Charge Storage. Consider again the capacitor system that was described in Figs. 1 and 2. When the battery of potential V is connected across the plates the electric field E between

the plates is uniform. This field arises from electrical charges on the internal surfaces of the metal plates, one positive and the other negative, each of density σ_0 per unit area. The magnitude of charge on each plate is $Q = \sigma_0 A$. On substituting for the capacitance we have

$$Q = \sigma_0 A = V\epsilon_0 A/d = CV \tag{5}$$

where

$$\sigma_0 = E\epsilon_0 \tag{6}$$

The dielectric polarizes in the field and annuls a fraction of the plate charge. As indicated earlier, the potential source replaces this charge with an additional component σ_p in order to reestablish equilibrium, and the field within the dielectric remains at the original value, $E = V/d$. At this point the internal polarization has generated surface charges within the dielectric of magnitude σ_p. The total charge stored on each plate, per unit area, is

$$\sigma_p + \sigma_0 = \epsilon_0 \epsilon_r \sigma_0 \tag{7}$$

and the equivalent charge densities at the surfaces of the dielectric are

$$\epsilon_r \sigma_0 - \sigma_0 = (\epsilon_r - 1)\sigma_0 = \chi_r \sigma_0 \tag{8}$$

where χ_r is the dielectric susceptibility of the dispersion processes in the dielectric that have responded to the action of the field. That is, those with polarization relaxation times less than the time of observation, and the difference between ϵ_r and χ_r over the complete frequency spectrum is the free-space relative permittivity of magnitude 1.0.

The additional charge stored is the polarization charge of magnitude σ_p per unit area. Considering the capacitor as a charge storage device we require a large electrode area and a high permittivity in order to store significant charge and a high internal impedance in order that the charge should not leak away internally through the dielectric. The impedance of the dielectric is in parallel with the capacitance and the intrinsic relaxation time for the stored charge can be obtained by consideration of the decay time of the equivalent parallel resistance–capacitance circuit. The time constant for the internal decay of the charge on removal of the voltage source and leaving the capacitor as an open circuit is given by the product of the parallel resistance and capacitance of the dielectric, that is,

$$\tau_{\text{int}} = RC = \frac{d\rho_r}{A}\frac{\epsilon_r A}{d} = \epsilon_r \rho_r \tag{9}$$

where ρ_r is the dc resistivity of the dielectric. The intrinsic relaxation time is independent of the geometry of the capacitor and, for example, with $\epsilon_r = 2$ and a relaxation time of a year, the resistivity has to be greater than $2 \times 10^{18}\ \Omega \cdot \text{m}^{-1}$, which is not a significant limitation since good insulators are designed to achieve this value. It is because of their long relaxation times that dielectrics have a useful charge-storage role. The density of the charge stored can be increased by raising the magnitude of the permittivity. In this context ferroelectric dielectrics (2), which have anomalously high permittivities, up to the order of thousands, play a major role.

Polarizability. All solids are comprised of individual atoms or molecules. The bonding of these elements is invariably electrostatic in the sense that common salt, sodium chloride, is a hard, clear crystal in which the sodium and chlorine atoms are ionized and result in strong, local fields and significant polarization, but the individual dipoles cannot approach one another by a distance that is less than their physical lengths. Averaging the electric fields within the bulk on a scale that is small but greater than that of the dipoles gives only the applied field as the effects of the local perturbations are lost.

The classic approach to polarization is to determine the effect of the local electric field acting on a dipole. Computing techniques make it a simple matter to explore the local charge densities by filling a dielectric with identical dipolar entities that are aligned by the electric field established across the sample, but leaving one, central, dipolar site empty. Two frames from a time development of two such models is shown in Fig. 3. Figures 3(a) and 3(c) refer to short times in the development of equilibrium and Figs. 3(b) and 3(d) to the equilibrium situation. In Figs. 3(a) and 3(b) we consider the interior of the dielectric in which the dipoles migrate randomly and we sample points at random within the dielectric bulk. In the equilibrium situation only the surfaces adjacent to the electrodes develop a net space charge as indicated. In Figs. 3(c) and 3(d) we consider the case for which the monitoring point is set at the center of one of the dipoles that has been chosen to be at the center of the sample area. The other dipoles are also contained within their molecules so that the area of twice the molecular radius is excluded from the general dipolar noise. However, the surface of the excluded area acts as an internal interface, which gives rise to an additional field component which is uniform within the enclosed volume, Fig. 3(d).

In a polarized material the vector electric field is given by

$$\boldsymbol{E} = \boldsymbol{E}_0 + \boldsymbol{E}_p \tag{10}$$

where $\boldsymbol{E}_0$ is the applied field, and $\boldsymbol{E}_p$ is the field generated by the polarization. We consider that each individual polarizable entity has a polarizability of magnitude $\alpha\epsilon_0$ so that the total polarization is

$$\boldsymbol{P} = \frac{N_a \rho \alpha \epsilon_0}{M} \quad E_{local} \tag{11}$$

$$= \epsilon_0(\epsilon_r - 1)\boldsymbol{E}_0 \tag{12}$$

where N_a is Avogadro's number, ρ is the density of the material of molecular weight M and E_{local} is the local electric field. Considering that a small spherical volume surrounds each polarizable molecule, the local electric field at the molecule is given by

$$E_{local} = \left(1 + \frac{\epsilon_r - 1}{3}\right) E_0 \tag{13}$$

From Eqs. (12) and (13) we have that

$$\alpha\epsilon_0 = \frac{3\epsilon_0}{N_a \rho} M \frac{\epsilon_r - 1}{\epsilon_r + 2} \tag{14}$$

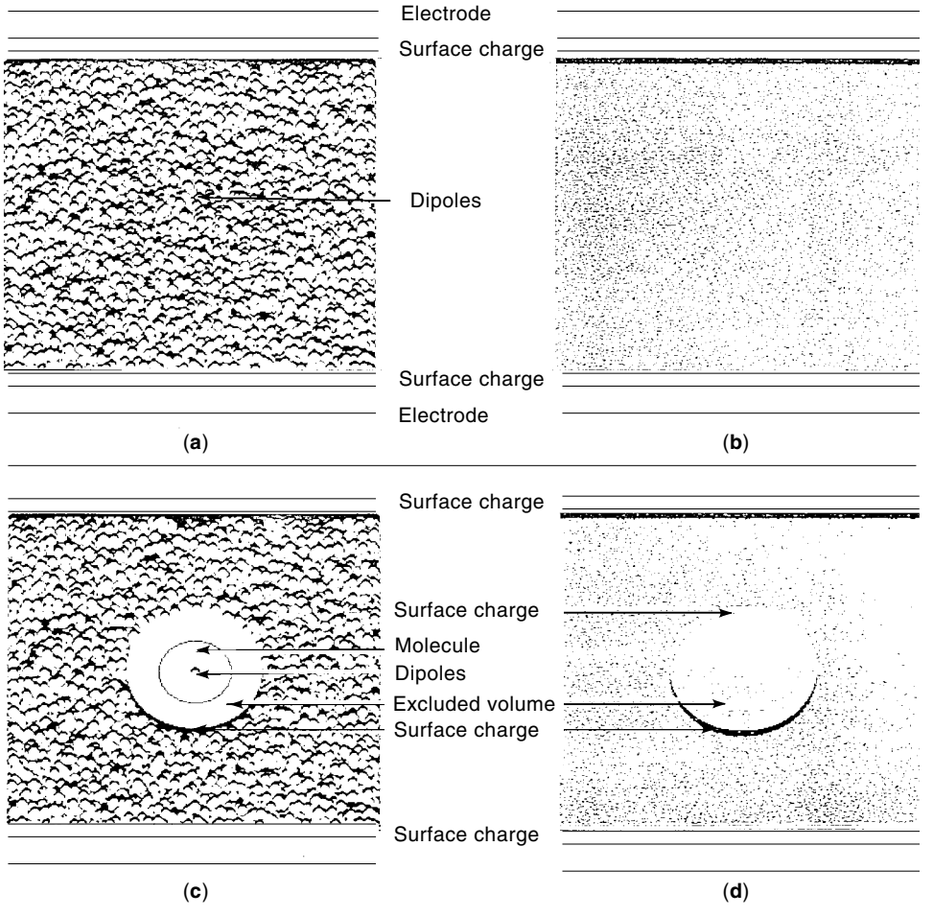

Figure 3. In a gas, liquid, or solid, with no field present, on average the dipoles are randomly distributed, leading to zero charge density everywhere. On the application of an electric field surface charges are formed in the material adjacent to the electrodes. However, the charge density surrounding a fixed dipole, taken to be at the center of the sample, is not the same as the average value. The molecular diameters exclude a volume of radius twice the molecular radius. At the surface of the excluded volume a surface charge is generated, similar to those at the electrodes. In the diagrams panels (b) and (d) show the equilibrium state and (a) and (c) the summations of the local polarizations before equilibrium has been achieved. The charge cloud surrounding the fixed dipole is equivalent to that generated on the surface of a similar void in the dielectric.

which is the well established Clausius (2)–Mosotti (3) relationship. Structurally complex molecules will have larger values for their equivalent molecular radii and hence larger polarizabilities. Table 2 lists the magnitudes of the polarizabilities for a small number of ions and molecules from which it can be seen that the range of polarizabilities is large and dependent on the molecular size and content, to a significant degree.

DIELECTRIC DISPERSION

Our description so far has been in terms of the equilibrium macroscopic response of the dielectric and has not considered the time dependence of the polarization. It is expected that even in a perfectly homogeneous dielectric the individual charged components that constitute the dipoles and given the internal polarization will each contribute to the total response and that each will respond in its own time scale. In principle, information about these processes can be extracted from an experiment that measures the time dependence of the decay of polarization of a charged sample. However, such measurements are dynamic over an extended time scale and it is only since fast information retrieval and storage systems have been developed that direct measurement of the time decay has become an effective technique. The alternative approach is to use a variable-frequency ac voltage source and choose a suitable set of frequencies within the range of the source, and then at each of these frequencies allow dynamic equilibrium to be achieved and to measure the in-phase and out-of-phase components of the response to the applied ac voltage. The advantage in this technique is that the material under study reaches a dynamic equilibrium at the chosen frequency so that repeat measurements can be made until the variations in the measures are at an acceptable low value. In this case the data are conventionally expressed in terms of either the

Table 2. Polarizabilities (in units of $C \cdot m^2 \cdot V^{-1}$)[a]

Ion/molecule	Na^+	Cl^-	NH_3	C_2H_6 Ethane	C_6H_6 Benzene	C_6H_{14} Hexane
Polarizability	0.22	3.3	2.56	5.0	11.46	13.1

[a] Polarizabilities are not often quoted in the relevant SI units, which are 10^{-16} C · m² · V⁻¹. The values are normally listed in cgs units of cm^3. The conversion factor is

$$\alpha_{SI} = 1.113 \times 10^{-16} \alpha_{cgs}$$

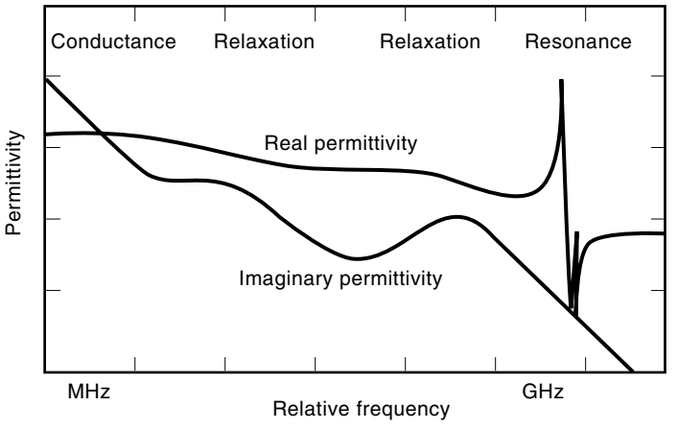

Figure 4. A schematic diagram of the dispersion of the real, $\epsilon'(\omega)$ and imaginary $\epsilon''(\omega)$, components of the complex permittivity. The frequency range covers, from right to left the optical, microwave, radio, and low frequency ac spectrum equivalent to the frequency range from 10^{15} to 10^{-3} Hz. In order to cover this extended frequency range logarithmic frequency and permittivity scales have been assumed. At the lowest frequencies a bulk conductance component dominates the dielectric loss but makes no contribution to the real component of the permittivity. Note the sharp maximum in the loss at the resonant frequency.

capacitance or the permittivity for which the proportionality between these properties is a dimensional constant dependent only on the sample geometry, Eq. (2a).

A sketch of the in-phase and out-of-phase, the real and imaginary, components of the permittivity as a function of frequency is presented in Fig. 4 in which we indicate a resonance response at high, typically optical frequencies and two broad relaxation responses in the MHz and kHz regions with, at the lowest frequencies, a contribution to the imaginary component of the permittivity from the dc conductivity of the sample. It should be noted that in the figure we have assumed logarithmic scales that is, log (permittivity) as a function of the log(frequency) as both the frequency–magnitude range and the permittivity range are large and the log scales retain a uniform sensitivity throughout these ranges as well as compressing the absolute value scales.

The frequency-scan technique is a convenient means of quantifying the relative magnitudes and of characterizing the nature of the individual dispersion processes; resonances are of narrow frequency range with characteristic maximum and minimum in the real component and a narrow absorption peak in the out-of-phase (energy absorption or loss) component. A narrow energy-loss peak is one in which the width at half the peak height is significantly less than one order of magnitude and usually much less. Damping of a resonance increases the frequency range of the loss component and overdamping drives the system into relaxation. Relaxation peaks are much broader with a minimum half-height width of greater than one order in magnitude. The two responses in the midfrequency range of the figure are both relaxations with the lower-frequency loss peak significantly broader than that at the higher frequency, which is a common experimental observation.

As the dielectric response is delayed with respect to the applied voltage it can be considered as a vector rotating at the same rate as the ac voltage but delayed in phase. In this form we have, in complex algebra notation,

$$\epsilon(\omega\tau) = \epsilon'(\omega\tau) - j\epsilon''(\omega\tau) \tag{15a}$$

$$= \epsilon_r \exp(-j\,\omega\tau) \tag{15b}$$

$$= \epsilon_r[\cos(\omega\tau) - j\sin(\omega\tau)] \tag{15c}$$

The imaginary component of the dielectric response $\epsilon_r \sin(\omega\tau)$ is an electrical current and is defined to be in phase with the applied voltage, which results in energy loss as heat in the material. For this reason the real component of the permittivity represents the capacitively stored charge and the imaginary component is termed the dielectric loss.

At the lowest frequencies the real component of the capacitance is constant and nondispersive, while the loss component increases as the inverse of the frequency, ω. The magnitude of the ac conductance of a capacitor of magnitude C, in complex notation, is $i\omega C$. From this we see that the contribution to capacitance of the conductance of magnitude G is $C_g = -jG/\omega$, giving the inverse frequency dependence of the dispersion in the loss, indicated in Fig. 4. Resonance normally occurs at very high, that is, quasioptical, frequencies whereas at cable transmission frequencies the loss is dominated by broad relaxation loss peaks and dispersions in the real component of the permittivity. The out-of-phase component in these peaks acts as an electrical impedance in phase with the applied voltage and hence passes energy to the dielectric as heat, in precisely the same manner as the low-frequency conductance. However a perfect conductance possesses no capacitance and hence there is no dispersion in the real component.

As indicated in Fig. 4, the observed permittivity is frequency dependent. The diagram also shows that when more than one process exists, the real permittivity at frequency ω, $\epsilon'(\omega)$, is the summation of the contributions for all frequencies greater than ω. We can write this as $\epsilon(\omega) = \sum\chi_s(\omega)$ over all s, where the contribution of the sth component is the susceptibility $\chi_s(\omega)$, and the $s = 0$ terms gives the "free-space" contribution of 1.0.

Dielectric relaxation has been observed from very low frequencies, μHz, to high GHz, frequencies, but there is always an additional contribution to the permittivity from the optical region, as indicated by the resonance process in Fig. 4. For example, the permittivity of optical glass is 6 in the kilohertz range and the optical refractive indices are about 1.5. The refractive index is the ratio of the velocity of light in the vacuum to that in the medium, and the equivalent, optical susceptibility is the square of this ratio, 2.25 and includes the relativity permittivity of free-space. The permittivity of optical glasses in the kilohertz frequency range is about 6, and hence we know that one or more dispersion processes is required between the optical frequency range and the kilohertz range, of total magnitude 3.75 in relative susceptibility. Natural quartz has a refractive index of 1.55, but the kilohertz permittivity is only 4.5, and hence the equivalent midfrequency residue is reduced, in quartz, to 2.1. We can associate the difference between quartz and glass to the introduction of metal ions, which make the optical glasses easier to manufacture. It is common to consider the summation of responses at frequencies higher than that of particular interest to an observer as an infinite frequency permittivity to which

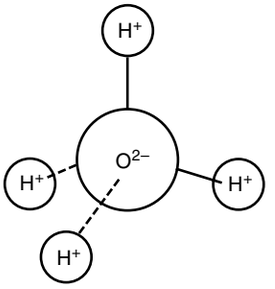

Figure 5. The H_2O (water) molecule. Each of the four bonding directions are at 100° to the others and two of the four bonding positions will be occupied by two hydrogen H^+ ions. The equivalent negative charge is given by the oxygen O^{2-} ion at the center and the polarization vector lies from the central core to a position midway between the hydrogen ions. A change in position of one hydrogen ion gives a realignment of the polarization vector by 100° and occupation of the initially empty *pair* of sites by the hydrogen ions reverses the initial polarization.

we give the symbol ϵ_∞. In the case of the glasses we can define ϵ_∞ for the dielectric, kilohertz, range as about n^2_{optical} (i.e., 2.25).

The experimental observation that the individual relaxation–resonant processes add together independently, as assumed in Eq. (15), is the basis of the principle of superposition, which states that the individual polarization processes are additive and, by implication, negate the possibility of coupling, in any form, between these processes. Experimentally the principle of superposition applies as long as the individual dispersion responses are linear with respect to the applied field.

In all cases the basis of the observed permittivity is the realignment of charges within the material under the action of an externally applied electric field. As a classic example of a simple molecule and the nature of its dielectric response we may consider the water molecule, H_2O. The hydrogen atoms are negatively charged and the oxygen positively double charged so that although the molecule is electrically neutral it contains two simple dipoles aligned along the bonding directions, which give a resultant dipole to the molecule. This arises because there are four, equivalent directions forming angles of 100° to each other, centered on the oxygen O^{2-} ion for the two hydrogen ions, and at any one time two of these positions are occupied, as indicated in Fig. 5. This results in a net dipole for the molecule the direction of which bisects the angle between the two occupied hydrogen positions. If one of the pair of hydrogen ions moves to either one of the empty allowed sites there is a concomitant 100° shift in the direction of the dipole. In thermal equilibrium, and at zero applied electric field, the hydrogen ions move from site to site within the molecule at random, and the net polarization, given as the average over an ensemble of molecules with random directions of polarization, is zero. However, once an electric field is applied more of the dipoles will be aligned in the field direction and the material will become polarized. Thermal randomization opposes the field-driven polarization and a dynamic equilibrium is established. For small fields the polarization is a small perturbation in the material and, as indicated by Eq. (14), we can write

$$P = \boldsymbol{m} \cdot \boldsymbol{E} \tag{16}$$

where P is the net polarization, $\boldsymbol{E}$ the electric field, and $\boldsymbol{m}$ the dipole moment of the molecule. The structure of the water molecule is such that it is easily polarized and results in the anomalous high permittivity listed in Table 1. Conversely the long intermeshed and tightly bound hydrocarbon chains typical of polymers are unable to allow significant ion movement under equivalent fields and hence their polarizabilities, and permittivities, are small.

Dielectric Relaxation

The availability of wide-band, automatic measuring machines for low frequency since the early 1980s has brought about the development of wide-band dielectric spectroscopy as an effective tool for the physical investigation of poorly conducting solid and semisolid materials. At the same time the long established chemical interest in polar molecules has been strengthened by advances in data measurement, storage, and analysis. Now that high-quality high-resolution data are widely available, it is essential that the fundamental background to these observations is made clear in order to ensure that the experimental data are analysed in the most effective manner.

Following Kubo (4) we define the form of the relaxation dispersions in frequency, through the time response of the system after the application, or removal, of an electric field. The time dependence of the polarization $P(t)$ following the application of an electric field, $E(t)$, is given by

$$P(t) = \epsilon_0 \int_{-\infty}^{t} \phi(t - t') E(t')\, dt' \tag{17}$$

where $\phi(t)$ is the linear response function and ϵ_0 is the permittivity of free space. For "small" magnitudes of the applied field, as indicated earlier, the response of the polarization is taken to be a linear function of the magnitude of the applied field. The function $\phi(t)$ is required to be real and to approach zero as t tends to infinity. In practice the limitation to small fields is not restrictive as the local fields within most solids are high and the external fields normally used in dielectric spectroscopy result in small perturbations. For the specific case where the electric field is sinusoidal, with angular frequency ω, the field is

$$E(\omega, t) = E_0 \exp(-j\omega t) \tag{18}$$

and the polarization can be written in the form

$$\begin{aligned} \Delta P(\omega t) &= \epsilon_0 E_0 \int_{-\infty}^{t} \phi(t - t') \exp(j\omega t')\, dt' \\ &= \epsilon_0 E_0 \exp(i\omega t) \int_{-\infty}^{t} \phi(t - t') \exp[-j\omega(t - t')]\, dt' \\ &= \epsilon_0 E_0 \exp(i\omega t) \int_{0}^{\infty} \phi(T) \exp(-j\omega T)\, dT \end{aligned} \tag{19}$$

which is the Fourier transform of the response function $\phi(T)$ and gives the susceptibility as

$$\begin{aligned} \chi(\omega) &= P(\omega)/(E_0\epsilon_0) = \int_0^\infty \phi(t') \exp(j\omega t')\, dt' \\ &= \chi'(\omega) - i\chi''(\omega) \end{aligned} \tag{20}$$

Applying the principle of superposition to a linear system that contains N independent relaxation processes, the overall response function is

$$\phi(t) = \sum_{s=0}^{N} \phi_s(t) \tag{21}$$

where $\phi_s(t)$ is the response of the sth relaxation process. Substitution then gives the complex permittivity in the form

$$\epsilon'(\omega) - i\epsilon''(\omega) = \epsilon_0 \left(\sum_{s=1}^{N} \phi_s(t) \exp(j\omega t) + 1 \right) \tag{22}$$

In addition to the time-decay response most materials exhibit a small dc conductance, which has no time-decay function. The conductance gives an additional component to the loss mechanism, as indicated in Fig. 4, adding to the permittivity a term $-j\sigma\omega^{-1}$, where σ is the conductivity of the sample.

The ratio of the real to the imaginary component of the complex permittivity defines the phase difference between the response and the applied voltage. For zero phase difference the material acts as a perfect resistance and dissipates power. For a phase difference of $\pi/2$ the response is out of phase with the driving potential and no energy is lost. The phase angle δ is a measure of the fraction of energy lost as heat and not available for use and is defined by

$$\epsilon''(\omega)/\epsilon'(\omega) = \tan(\delta) \tag{23}$$

For this reason δ is commonly termed the loss angle and is used to characterize the electrical quality of the material.

Kramers–Kronig Relationships. Separating out the real and imaginary components of the complex susceptibility, from Eqs. (20) and (21) we have

$$\chi'(\omega) = \epsilon_0^{-1} \int_0^{\infty} \cos(\omega t)\phi(t)\, dt \tag{24}$$

$$\chi''(\omega) = \epsilon_0^{-1} \int_0^{\infty} \sin(\omega t)\phi(t)\, dt \tag{25}$$

Fourier inversion of the second of these equations gives

$$\phi(t) = \epsilon_0 \frac{2}{\pi} \int_0^{\infty} \sin(st)\chi''(s)\, ds \tag{26}$$

so that after substitution into Eq. (24) we obtain

$$\chi'(\omega) = \frac{2}{\pi} \int_0^{\infty} \int_0^{\infty} \chi''(s)\, \sin(st)\, \cos(\omega t)\, ds\, dt \tag{27}$$

Brot (5) has expressed the double integral in the form

$$\chi'(\omega) = \frac{2}{\pi} \lim_{r\to\infty} \int_0^{\infty} \frac{ds\, \chi''(s)}{2} \times \left(\frac{1}{s+\omega} + \frac{1}{s-\omega} - \frac{\cos(s+\omega)r}{s+\omega} - \frac{\cos(s-\omega)r}{s-\omega} \right) \tag{28}$$

but, as the last two terms in the large parentheses are oscillatory and $\chi''(\omega)$ is required to decay to zero as the frequency approaches infinity, we need only consider the first pair of terms. Hence we obtain

$$\chi'(\omega) = \frac{2}{\pi} \int_0^{\infty} \chi''(s) \frac{s}{s^2 - \omega^2}\, ds \tag{29}$$

$$\chi''(\omega) = \frac{2}{\pi} \int_0^{\infty} \chi'(s) \frac{\omega}{\omega^2 - s^2}\, ds \tag{30}$$

which are the Kramers (6)–Kronig (7) relationships between the real and imaginary components of the susceptibility. These relationships always apply, for the complex-frequency dependencies arise from a single, real, time-decay function. An immediate consequence of the relationships is that it is not possible to have a dispersion in one component without a related dispersion in the other unless $\chi''(\omega)$ has an ω^{-1} dependence in which case Eq. (29) contributes to zero to the magnitude of $\chi'(\omega)$.

A particular case, which we shall later show as of significance in the analysis of the dielectric response of many real materials, is that when either component of the susceptibility exhibits the fractal property of a fractional power decay with increasing frequency. Consider, as an example, that the real susceptibility can be expressed as

$$\chi'(\omega) = \chi_0 \omega^{-p} \qquad \text{with} \qquad 0 < p < 1 \tag{31}$$

and that p is fractional and positive over a reasonable frequency span. Substitution into Eq. (29) gives the imaginary loss component as (8)

$$\chi''(\omega) = \chi_0 \frac{2}{\pi} \omega^{-p} \int_0^{\infty} \frac{x^{-p}}{1 - x^2}\, dx = \chi_0 \omega^{-p} \cot(p\pi/2) \tag{32}$$

where $x = \omega/s$. We can reexpress Eq. (32) as

$$\chi''(\omega)/\chi'(\omega) = \tan[(p-1)\pi/2] = \text{const} \tag{33}$$

over the frequency range over which Eq. (31) applies. The angle $(p - 1)\pi/2$ in Eq. (33) is known as the phase angle of the loss or simply the loss angle for the dielectric and is a direct measure of the fraction of the energy lost as heat by way of the relaxation process.

Comparing Eq. (33) with Eq. (23), we note that the former applies for a single relaxation process and the latter for the summation of all relaxation and charge transport processes in the material with relaxation times less than the inverse of the frequency that is being considered. To a cable designer, the latter is more significant.

When the response is of a negative fractional power-law form, as is commonly observed in many dielectric materials, the dispersion spectra are characterized by a constant phase-

angle response for frequencies in excess of the relaxation time. An equivalent response can occur in the lower-frequency region, that is, in the region below the peak in the imaginary component, but in this case we have

$$\chi(0) - \chi'(\omega) = \chi''(\omega)\cot(p\pi/2) \tag{34}$$

As the Kramers–Kronig transform of either a constant term, or an inverse frequency dependence, is zero, the Kramers–Kronig interrelationships are useful in the analysis of experimental dispersion data, particularly when a conductivity of similar magnitude to that of the permittivity response is under consideration. The contribution to the sample of a conductivity is

$$\chi\sigma = -j(\sigma/\omega) \tag{35}$$

which on transformation is zero. In this manner the conductivity free permittivity can be determined by transforming the data containing the conductivity and then retransforming back and subtracting from the original data.

With the general usage of fast computing techniques the Kramers–Kronig transform has become freely accessible. However, in order to have effective transformations it is essential that the input data are both of high quality and of sufficient quantity to give an acceptably low scatter to the output of the computation.

DISPERSION FUNCTIONS

The principal feature of dielectric spectra below the GHz range is the total absence of resonance effects. The energy stored by polarization, in all solid and liquid media, relaxes under over damped conditions on time scales of greater than picoseconds and resonance effects, which are characterized by sharp, optical spectralike lines, have not been observed in the frequency range from microhertz to gigahertz. The simplest form of overdamped response is that for which the driving force for the relaxation of any forced displacement is due to the displacement itself, that is, in terms of the linear response function a first-order response with

$$\phi(t) = -\tau\frac{d\phi(t)}{dt} \tag{36}$$

where τ is a constant with dimensions of time and termed the relaxation time for the particular susceptbility process under consideration. Setting the magnitude of the polarization at zero time to be ϕ_0 the subsequent polarization decays exponentially as

$$\phi(t) = \phi_0\,\exp(-t/\tau) \tag{37}$$

The Fourier transform of the exponential time decay gives the frequency response of the polarization, where $P(\omega)$ is $\chi(\omega)E(\omega)$ and $\chi(\omega)$ is the dielectric susceptibility. Following Debye (9) and carrying out the Fourier transformation of Eq. (37) yields

$$\chi(\omega\tau) = \phi_0\frac{1}{1+i\omega\tau} = \phi_0\frac{1-i\omega\tau}{1+\omega^2\tau^2} \tag{38}$$

and, after separating out the real and imaginary complex components, we have

$$\chi'(\omega\tau)/\phi_0 = \frac{1}{1+\omega^2\tau^2}, \quad \chi''(\omega\tau)/\phi_0 = -\frac{\omega\tau}{1+\omega^2\tau^2} \tag{39}$$

hence for $\omega\tau < 1$

$$\chi'(\omega\tau) \simeq 1, \quad \chi''(\omega\tau) \simeq 1/\omega\tau \tag{40a}$$

and for $\omega\tau > 1$

$$\chi'(\omega\tau) \simeq 1/(\omega\tau)^2, \quad \chi''(\omega\tau) \simeq 1/\omega\tau \tag{40b}$$

The Debye relaxation can be characterized by the ratios of the frequencies for which the out-of-phase component is one-half and one-quarter of the magnitude of the total response, ϕ_0. For convenience in the following we assume that $\phi 0$ has a value of unity. The maximum in the loss component $\phi''(\omega\tau)$ is half the total real dispersion and occurs for the $\omega\tau = 1.0$ and the ratio of frequencies for which the latter applies is 1 : 10.194, that is, just over an order in magnitude, as shown in Fig. 6. In this figure we have presented, as functions of the frequency, the response in linear and logarithmic scales together with the Cole–Cole (10) presentation of $\chi''(\omega\tau)$ as a function of $\chi'(\omega\tau)$. In Figs. 6(a), 6(b), and 6(c) it is clear that the loss peak is symmetrical on a log(frequency) scale as is implicit in the form of Eq. (36), and that the peak value of the loss component is one-half of the zero-frequency magnitude of the dispersion. The second feature of the plot is that outside of a relatively narrow range of frequencies centered on $\omega = 1/\tau$ the dispersions of $\chi'(\omega)$ are simple, in the sense that the frequency exponents are whole numbers, including zero, that is, $\xi\omega\tau$, $(\omega\tau)^{-1}$, $(\omega\tau)^{-2}$, and $1 - \omega\tau$.

In practice the precise form of the Debye response is seldom observed. Invariably both solid and liquid dielectrics exhibit a significant broadening of the Debye relaxation characteristic. The cases for which perfect Debye behavior might be expected are for low concentrations of a polarizable entity dispersed uniformly in a nonpolar medium such as a gas at low pressures or polarizable atoms or ions evenly dispersed in a polymer host but not bound into the polymer chains. Water and deuterium oxide approximate closely to the Debye form, within the accuracy with which the measurements can be carried out. For water at room temperature the relevant dispersion processes occur in the GHz region of the electromagnetic spectrum, which is experimentally a difficult region in which to obtain data over a broad frequency range. In practice the variation from the Debye response is of essentially of the same order of magnitude as the variation in the measurements themselves. In Fig. 7 we present the form of the water dispersion measured, with a high accuracy, by Alison (11), Richards (12), and Alison and Sheppard (13) and note that the data indicate a small, but real, variation from the Debye form for $\omega\tau > 1$ ($\omega \geq 10^5$ MHz). We also note that above this frequency the real and imaginary components deviate from the Debye form and tend to become parallel in the log–log plot; hence Eq. (33) applies with $p = 1 - n$ and the value of the gradient was determined by the authors as $n = 0.043 \pm 0.001$.

Examination of some 200 sets of published experimental data (14) has shown that the Debye exponents are limiting

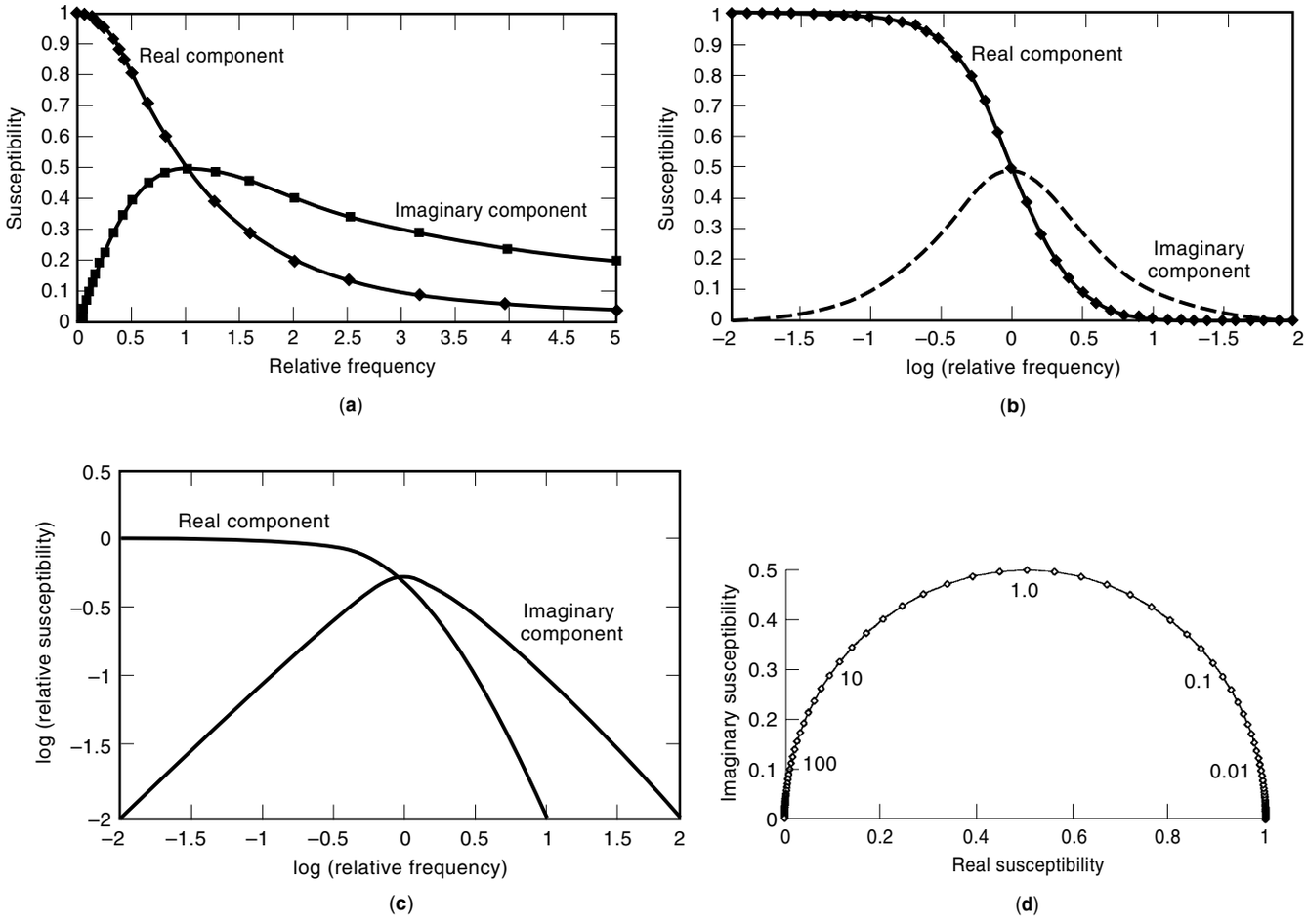

Figure 6. The Debye dispersion function components $x'(\omega)$ and $x''(\omega)$ for $x_0 = 1.0$ is plotted using (a) linear scales, (b) log–linear scales, and (c) logarithmic scales in order to show the symmetry of the loss component with log(frequency). In (d) the Debye data are plotted as the imaginary permittivities as a function of the real permittivities and give the Cole–Cole semicircle. The numbers in the plot indicate relevant $\omega\tau$ values.

values and only approached by a small fraction of the materials investigated. Figure 8 contains a plot of the exponents in terms of the relevant loss peaks in terms of the Jonscher (15) notation, which for $\omega\tau < 1$,

$$\chi''(\omega\tau) \propto \omega^m$$
$$\chi'(\omega\tau) \propto 1 - \omega^m, \qquad 0 < m \leq 1.0$$

and for $\omega\tau > 1$,

$$\chi'(\omega\tau) \propto \chi''(\omega) \propto \omega^{n-1}, \qquad 0 \leq n < 1.0$$

The Debye characteristic is indicated in the diagram as a single point with coordinates ($m = 1$, $n = 0$). The origin of the plot is the point, ($m = 0$, $n = 1$), which represents zero dispersion with a constant real susceptibility over the relevant frequency range, and as a consequence of the Kramers–Kronig transformation the equivalent loss component will have zero magnitude. It is obvious that the bulk of the dielectric data lies above the diagonal between these limiting values, that is, $m + n > 1$. In the figure two other recognized dispersion forms, the Cole–Cole (10) and Davidson–Cole (15) functions are indicated. In terms of the exponent parameters these functions require that $m + n = 1$ and $m = 1$, respectively. The form of these, and other recognized dispersion functions are listed in Table 3.

The plot contains preferred areas; generally polymeric materials are found close to the origin, $m \approx 0$, $n \approx 1$, whereas water and ice and D_2O as solid and liquid are close to the Debye value at (1,1), Fig. 7, and tend to lie on the Cole–Cole diagonal of the plot. The Cole–Davison function defines the upper frame of the figure as $m = 1$.

Two typical examples of dielectric dispersions are given in Fig. 9 as the general behavior patterns that have been observed. The legend to the figure contains the relevant dispersion parameters. Figure 9(a) shows the loss measured for the α relaxation process in linear polyethylene at a constant temperature of 363 °K as a function of the applied pressure (16). Increasing the pressure has had the effect of increasing the relaxation time without a significant change in the magnitude of the dispersion. The real permittivity for this set of data has a magnitude close to three and the

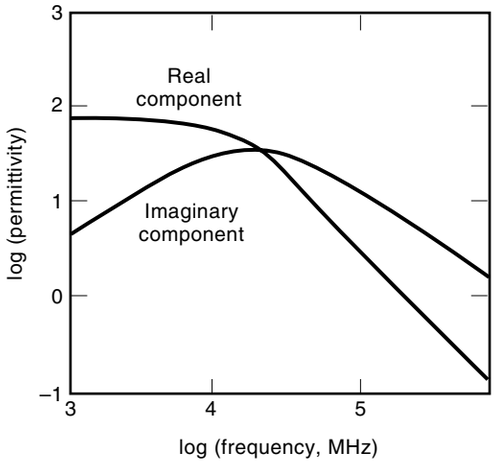

Figure 7. The dielectric dispersion of water at 23°C as reported by Alison and Sheppard (13). For clarity the plot in the figure is the fitted Cole–Davidson/Dissado–Hill function using the parameters $n = 1.001 \pm 0.001$ and $m = \beta_{CD} = 0.043 \pm 0.001$. These values were determined with a statistical certainty of $\chi^2/v = 1.5$ where $v = 683$ degrees of freedom.

increment in $\epsilon'(\omega)$ due to this relaxation was no more than 0.05 pF. Figure 9(b) contains both the real and imaginary components of a dispersion in polyvinyl acetate (17). The data were measured at three temperatures, and the fractional power behavior in the wings of the dispersion is clear and independent of the temperature. In this case we have $m = 0.80 \pm 0.02$, $1 - n = 0.56 \pm 0.02$ and the half-width is approximately two orders of magnitude, significantly wider that the Debye dispersion. The data presented in Fig. 9 has been chosen to be indicative of the range of dielectric response and of the influence of external variables and structure on the dynamics of relaxation.

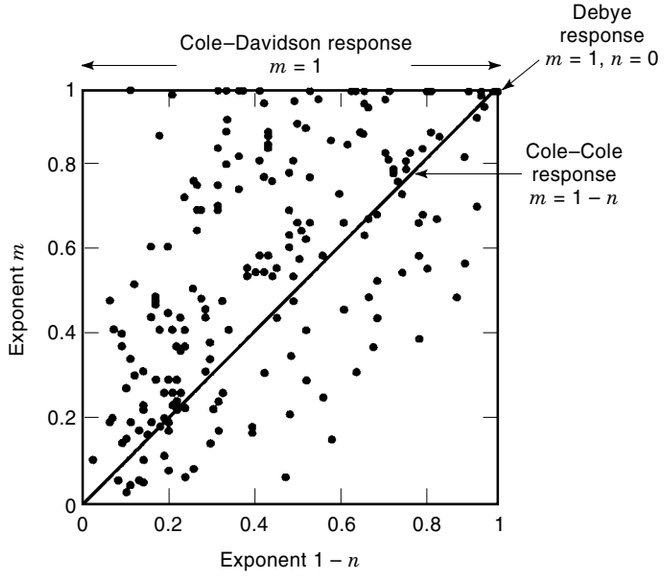

Figure 8. A plot of the low-frequency exponent for the loss m as a function of the magnitude of the high-frequency exponent, $1 - n$, for two hundred individual data sets taken from the published literature. One half of the data have been reported in Ref. 14. The regions of this plot for which the Debye, Cole–Cole, and Cole–Davidson dispersion functions apply are indicated.

It is clear that the Debye model is not of general applicability although the concept of a broad relaxation spectrum is fundamental. One approach to describe the observed relaxations has been to generate empirical relaxation functions, either in the time domain, see Eq. (37), or directly in the frequency domain. A number of the frequency dispersion functions are listed in Table 3 and, as indicated above, three of them have specific restraints and have been mapped onto the data plot of Fig. 8.

It is a feature of the functions at they all contain fractional power-law behavior in at least one of the wings of the response, whereas the experimental evidence in Fig. 8, clearly requires two parameters in order to have the necessary flexibility to mirror the experimental observations, for which we require for $\omega > \omega_{peak}$,

$$\chi''(\omega) \propto (j\omega)^{n-1} \propto \omega^{n-1} \sin(n\pi/2) \tag{41a}$$

$$\chi'(\omega) \propto \omega^{n-1} \cos(n\pi/2) \tag{41b}$$

and in the lower-frequency range, $\omega < \omega_p$,

$$\chi''(\omega) \propto (\omega)^m \sin(m\pi/2) \tag{42a}$$

$$\chi'(\omega) \propto [1 - \omega^m \cos(m\pi/2)] \tag{42b}$$

Table 3 shows that only the Havriliak–Negami (18), Jonscher (19), and Dissado–Hill (20) functions make use of two, independent, descriptors that are necessary in order to cover the range of experimental data covered in Figs. 5, 8, and 9. One other dispersion function has been reported in the literature, the Kohlrausch (21), Williams and Watts (22) function (KWW), which has been defined in terms of the time-decay function (21)

$$f(t) \propto \exp[-(t/\tau)^\beta] \tag{43}$$

No simple frequency transform of this function exists (23). Expansion of the exponential and transformation of the individual elements gives series, for both low and high frequencies, which are oscillatory and poorly convergent. In Fig. 10 we present typical examples of the form of the dispersion functions and it is clear that the KWW dispersion is of the Cole–Davidson form and as the dispersion parameter β becomes small, the limiting low frequency ω^{-1} loss characteristic moves down to the very-low-frequency range and the curvature around the peak loss extends over orders of magnitude in frequency.

Distributions of Relaxation Times

A second approach that has been developed to explain the smearing out of the loss peak was originated by Pellat (24). He considered that a number of individual relaxation processes could occur in parallel, each with its own relaxation time τ_S and magnitude $\chi(O)_S$. The observed response is then given by the summation of the individual terms as long as they do not interfere or cooperate with each other, that is, as long as the principle of superposition applied. Taking the

Table 3. Dispersion Functions[a,b]

Dispersion Function	Source	Comment
$F(\omega) = \dfrac{1}{1 + i\omega\tau}$	Debye (9)	
$F(\omega) = \dfrac{1}{1 + (i\omega\tau)^{1-\alpha}}$	Cole–Cole (10)	$\alpha \equiv m = 1 - n$
$F(\omega) = \dfrac{1}{(1 + i\omega\tau)^{\beta}}$	Cole–Davidson (15)	$\beta \equiv n - 1, m \equiv 1$
$F''(\omega) = \dfrac{\epsilon''_m}{(\omega/\omega_0)^{-\alpha} + (\omega/\omega_0)^{\alpha}}$	Fuoss–Kirkwood (31)	$\alpha \equiv m = 1 - n$
$F''(\omega) = \dfrac{\epsilon''_m}{(\omega/\omega_0)^{-\alpha} + (\omega/\omega_0)^{\alpha}}$	Havriliak–Negami (18)	$m \equiv 1, n \equiv 1 - \beta(1 - \alpha)$
$F(\omega) = -\beta \dfrac{\Gamma(s\beta)}{\Gamma(s)} \left(\dfrac{\exp(-i\pi\beta/2)}{(\omega\tau)^{\beta}} \right) s$	Kohlrausch–Williams–Watts (21,22)	
$F(\omega) = \dfrac{1}{(\omega/\omega_m)^{-m} + (\omega/\omega_n)^{1-n}}$	Jonscher (19)	
$F(\omega) = (1 + i\omega/\omega_0)^{n-1}\, {}_2F_1\left(1 - n, 1 - m; 2 - n; \dfrac{1}{1 + i(\omega/\omega_0)}\right)$ where ${}_2F_1(a, b; c; x)$ is the hypergeometric function	Dissado–Hill (32)	

[a] Each function has been normalized to unity susceptibility at zero frequency.
[b] The Fuoss–Kirkwood and Havriliak–Negami functions have been generalized by Jonscher using the m and $1 - n$ notation for the exponents of the low- and high-frequency wings, respectively. The Dissado–Hill function, which uses the same notation, is the only fundamentally based nonempirical response function and contains the Cole–Davidson function as a particular case. In the Dissado–Hill model n is the efficiency of energy exchange within a local cluster surrounding the active dipole and m is the equivalent efficiency for transfer of energy between clusters. All the dispersion functions include the Debye loss response as a specific case.

Debye dispersion as the model for a single perfect relaxor we can write

$$\chi(\omega) = \sum_S [\chi(0)_S (1 + i\omega\tau_S)^{-1}] \tag{44}$$

or, in the limit of a continuum of relaxation times

$$\chi(\omega) = \chi(0) \int_0^{\infty} \frac{G(\ln \tau)}{1 + i\omega\tau}\, d(\ln \tau) \tag{45}$$

in which $G(\ln \tau)$ is the preferred distribution function of the individual Debye relaxations on a logarithmic time scale with

$$\int_0^{\infty} G(\ln \tau)\, d(\ln \tau) = 1 \tag{46}$$

The distribution function can be obtained from the relaxation function using the relevant Stieltjes transform (21), however the information contained in $G(\ln \tau)$ cannot be more, and may be less, than that contained in the original dispersion plot. Only if the form of the relaxation distribution can be correlated with other information about a suitably distributed property of the system that could lead to the particular distribution is the technique of any real significance. Each of the dispersion functions listed in Table 3 may be recast into a distribution of relaxation times and Table 4 lists the relevant functions for which these have been determined. In the KWW case the transform is not simple, except for the case of $\beta = 0.5$ and the distribution of relaxation times has to be obtained by expanding $F(t)$ as a infinite power series and carrying out the transform for each term in the series. As the series $\beta \neq 0.5$ is generally oscillatory and poorly convergent we have chosen $\beta = 0.5$ as the KWW exponent in Fig. 11, where examples of the distributions obtained for single values of the variables are plotted. It can be seen the fractional power law in frequency transforms to an equivalent fractional power law in relaxation time and that the Cole–Davidson and KWW functions are represented by relaxation times limited to lower values, $\tau \leq 1.0$ and $\tau \leq 40$, respectively. It is reemphasized that no direct correlation between these Debye-based distributions and any other analysis of a distributed property within a dielectric has yet been reported. The distributions are mathematical transformations of the information contained in the frequency dispersion and hence of the relevant time-decay function and are of use as a guide to the spread of Debye relaxation times that would need to be involved. We note, however, that the concept of a distribution of relaxation times, although commonly used, depends on the absolute acceptance that any individual relaxing element in any environment will give a Debye relaxation. We consider that this is an extremely weak assumption and requires the total neglect of cooperative relaxations of any form. Indeed the functions listed previously are simply particular transforms of the essentially empirical dispersion functions in section in Table 3. Of these dispersion functions only one, the Dissado–Hill function, has been constructed *ab initio* from consideration of correlated relaxations on two different time scales. In this derivation it has been assumed that the time-decay function develops as a fractal process in time and that the fractional power laws in both the susceptibility and relaxation times are a direct consequence of the nature of the fractal correlations.

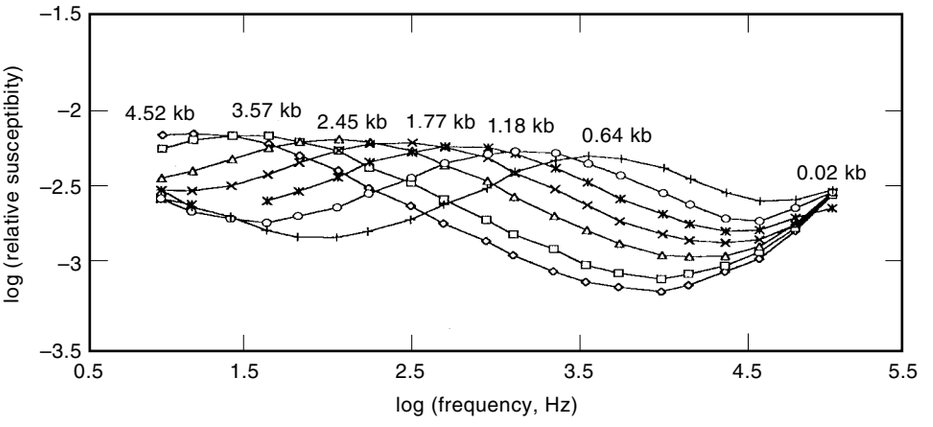

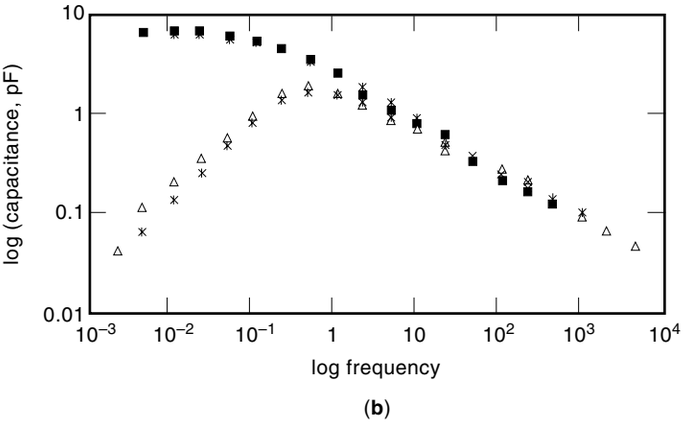

Figure 9. Two examples of typical dispersion plots. (a) Linear polyethylene under pressure (16). The pressure is indicated in the figure. T = 363°K. α relaxation. (b) Polyvinyl alcohol (17).

	G'	G''
317°K	■	△
322°K	×	*

It is with this concept, and its development, that there is evidence in support of the fractional power expressions assumed by the empiricists.

Quasi-dc Response

In the very-low-frequency region, which, for convenience, we will take as below 1 rad-s^{-1} (0.1592 Hz), the effect of conductance in the dielectric samples becomes important. For example a sample of area 1 cm^2, thickness 1 mm, and permittivity 20 has a capacitance of 120 pF. The equivalent resistance, at 1 rad/s frequency, is $8 \times 10^9\ \Omega$ and indicates a specific resistivity for the material of about $1 \cdot 2 \times 10^9\ \Omega \cdot \text{m}$.

A nondispersive conductance in the sample is characterized by a zero contribution to the real component of the permittivity and a contribution to the imaginary permittivity which is of an inverse frequency form, Eq. (35). However, if the loss component is almost but not *precisely* inversely proportional to the frequency, then there will be a contribution to the real component, and the ratio of the magnitudes of the individual components, the loss angle, *cf.* Eqs. (48), will be large with the consequence that the dispersion parameter can be determined with a high degree of accuracy.

For example, if we assume that the dispersion is of the form

$$\phi(\omega\tau) = \phi_0(j\omega\tau)^{\delta-1} \tag{47}$$

then the individual components are given as

$$\phi''(\omega\tau) = \phi_0(\omega\tau)^{\delta-1}\cos[\pi(\delta-1)/2] = \phi_0(\omega\tau)^{\delta-1}\sin(\delta\pi/2) \tag{48a}$$

$$\phi'(\omega\tau) = \phi_0(\omega\tau)^{\delta-1}\sin[\pi(\delta-1)/2] = \phi_0(\omega\tau)^{\delta-1}\cos(\delta\pi/2) \tag{48b}$$

$$\tan(\delta\pi/2) = \phi''(\omega)/\phi'(\omega) = \text{const} \tag{48c}$$

For δ approaching unity $\sin(\delta\pi/2)$ approximates to 1.0 and $\cos(\delta\pi/2)$ to zero. The characteristic defined by Eq. (47) is anomalous in that neither the real nor the imaginary component of the complex susceptibility saturates as the frequency becomes small and there is no equilibrium value for the ac response. Figure 12 shows an example of this anomalous dispersion and was observed by Giraud et al. (25) in a percolation system of mixed steel and glass balls of 30 μm diameter. The data were taken on the insulating side of the critical percolation density and, at the higher frequencies, show a strong conductance with the loss component, $\epsilon''(\omega\tau)$, inversely proportional to the frequency and accompanied by a strong dispersion in $\epsilon'(\omega\tau)$.

Data Presentation

The manner in which experimental data are best presented must be dependent on the purpose for which the data are to be used. There are three interrelated observables to report:

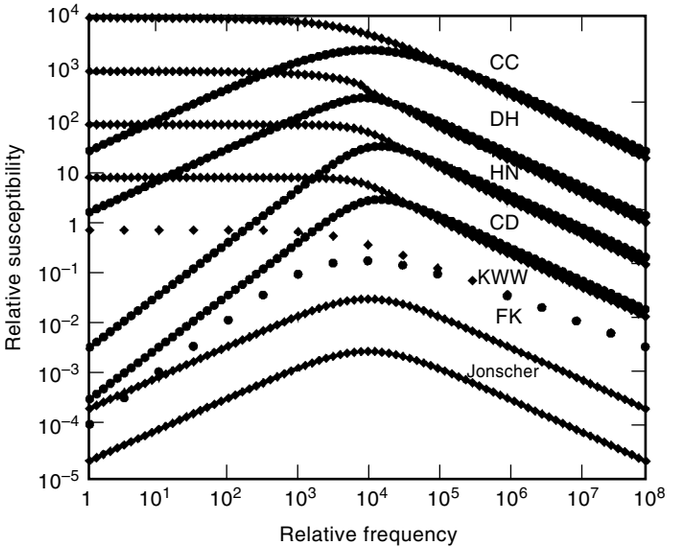

Figure 10. Examples of the forms of the Cole–Cole (CC), Dissado–Hill (DH), Havriliak–Negami (HN), Cole–Davidson, Kohlrausch–Williams–Watts (KWW), Fuoss–Kirkwood (FK), and Jonscher dispersion functions. The values for the variables are listed below and have been chosen to give as much compatibility between the plots as possible. CC, $\alpha = 0.4$; DH, $m = 0.6$ and $n = 0.4$; HN, $\alpha = 0.2$, $\beta = 0.75$; CD, $\beta = 0.6$; KWW, $\beta = 0.6$; FK, $\beta = 0.6$; Jonscher, $m = 0.6$ and $n = 0.4$.

Table 4. Distributions of Debye Relaxation Times (for convenience we have set $y = \omega\tau$.)

Function	$G\ln(\tau)$
Debye	δ function of magnitude 1.0 at $y = 1.0$
Cole–Cole	$(2\pi)^{-1}\dfrac{\sin(\pi\alpha)}{\cosh(1-\alpha)\ln(y)\} - \cos(\pi\alpha)}$
Cold–Davidson	$(2\pi)^{-1}\{[1+(y)e^{i\pi}]^{-\beta} - [1+(y)e^{-i\pi}]^{-\beta}\}$
Fuoss–Kirkwood	$\pi^{-1}\left(\dfrac{\alpha\cosh(\alpha\ln y)\cos(\frac{1}{2}\pi\alpha)}{\sinh^2(\alpha\ln y)+\cos^2(\frac{1}{2}\pi\alpha)}\right)$
Navriliak–Negami	$\pi^{-1}\left(\dfrac{y^{\beta(1-\alpha)}\sin(\beta\phi)}{(y^{2(1-\alpha)}+2y^{(1-\alpha)}\cos\pi(1-\alpha)+1)^{\beta/2}}\right)$
Dissado–Hill	$\dfrac{\sin(1-n)\pi}{\pi F_0}y^{-m}(1-y^{-1})^{n-m}\,{}_2F_1(1,n;1+m;y^{-1})$, $y \le 1$
	$\dfrac{\sin(m\pi)}{\pi F_0}\dfrac{1-n}{m}y^{-m}(1-y^{-1})^{n-m}\,{}_2F_1(q,n;1+m;y^{-1})$, $y \ge 1, F_0 = \Gamma(2-n),\Gamma(m)/\Gamma(1+m-n)$
Williams–Watts	The Williams and Watts has been defined, in the time domain, in terms of the step response function as $F(t) = \exp-(t/\tau_0)^{\beta}, \quad 0 < \omega < 1$ which can be expanded and transformed to give the relevant distribution function as a series summation. The function is weakly asymptotic to the final value and difficult to compute. For the particular case of $\beta = 0.5$ the exact solution is $(y/4\pi)^{1/2}\exp(-4y)$ (22).

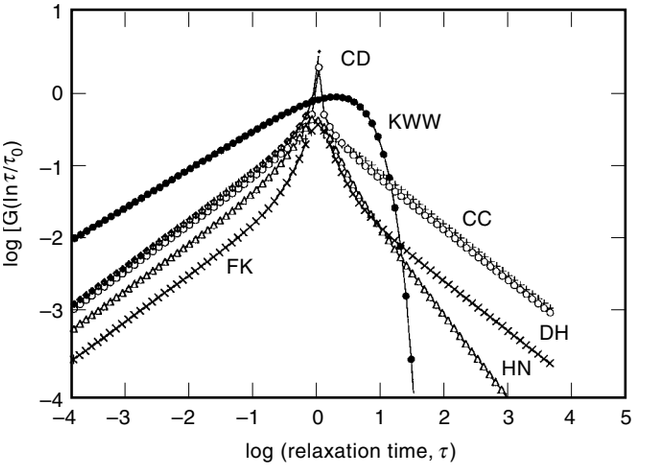

Figure 11. Examples of the distributions of Debye relaxation times for the range of functions listed in Table 4. The exponents used to obtain this plot are those listed in Fig. 10.

the real and imaginary components of the complex capacitance or permittivity as functions of the frequency. If the instrumental function is known, it is useful to report the data in terms of the relative permittivity for, as noted in the initial section, the magnitude of the permittivity contains information about the type of material being investigated. In particular, anomalously high values can well indicate that the sample is not homogeneous but internally structured.

In presenting data experimentalists should use the most effective and efficient technique of presentation and ensure that no information is lost. The recent development of best-fit analysis of data by computer calculation has the advantage, if all the information is reported, of allowing further reanalysis when, and as, more sophisticated data analysis techniques be-

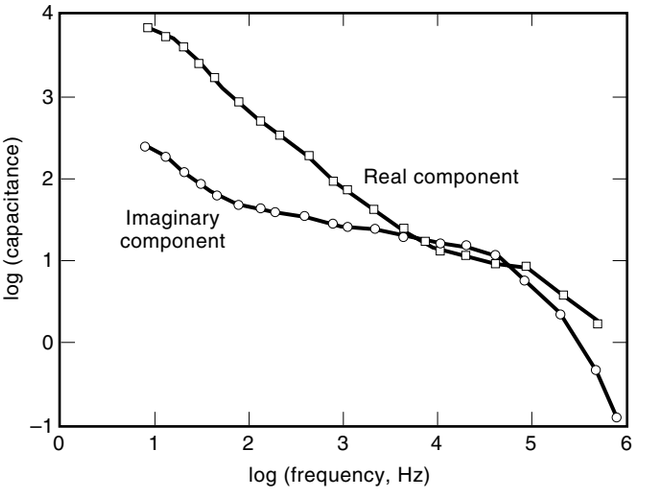

Figure 12. Dielectric response of a mixed metal and insulating system in the concentration region just below the percolation threshold. The bulk response, containing a well-defined conductivity dominates in the higher-frequency region. This response is truncated by a barrier layer. At lower frequencies the magnitude of the equivalent dielectric loss is less and the development of the dispersion in the real permittivity indicates a quasi-dc process with exponent $p \simeq 0.96$.

come available. Experimental data will be ignored if they are incomplete or inaccessible. In preparing Fig. 8, more than half of the data sets examined were rejected as they did not contain sufficient information to make an acceptable estimate of both exponents for the dispersion process that was reported.

As the processes being investigated are relaxations their half-widths will be in excess of an order in magnitude in frequency so that their examination suggests the use of a logarithmic frequency scales as indicated in Fig. 6. In this context we emphasize that all but one of the dispersion functions listed in Table 3 contain power-law responses as a consequence of the authors' independent observations that the bulk of the data that has been reported in the literature is of this form. It is therefore reasonable to use, as the initial data plot, logarithmic scales of either capacitance or permittivity as a function of the frequency in order to determine whether it does, or does not, indicate the general behavior pattern. The evidence from Fig. 8 is that the dispersion exponents refer in some way to the degree of order or cooperation within the individual materials, and it is noticeable that the glass transition temperature, which defines the change from the dominance of the α phase to the β phase of polymeric materials, can be characterized by a low half-width for the former and a large half-width for the latter in the dielectric response, that is, the α phase has $m \to 1.0$ and $n \to 0$ whereas in the β phase $m \to 0$ and $n \to 1.0$. Physically the α phase is associated with the more ordered backbone chains and the β phase with the more flexible side chains.

As indicated in Fig. 6(d) the Debye function can be plotted with $\chi''(\omega)$ as a function of $\chi'(\omega)$ on linear scales, the Cole–Cole plot, and results in a semicircular plot. Before broadband measuring equipment became available this was a reasonable technique of data presentation, for only a limited frequency range, around $\omega\tau = 1$, is required to define the semicircle. However, the limited frequency dependence in the wings of the Cole–Cole plot makes it practically impossible to recover experimental data, with any accuracy, from this form of presentation and hence further detailed analysis of the published data is, in practice, impossible.

For purposes of clarity log–log plots of the response as a function of the frequency are recommended. When an external variable is used, for example, temperature, the efficiency of information transfer is highest when *exactly* the same format of presentation is used across the full data set. It is commonly observed that the spectral form of the dispersions are not sensitive to the magnitude of the imposed variable, over at least reasonable ranges of magnitude. In these cases the quality of the data can be improved by rescaling the magnitude and frequency so that the individual plots can be stacked one on the other, giving a scale renormalization so that the data fit a single plot. An example of this technique is shown in Fig. 13 in which the original data from Fig. 9(a) have been renormalized and re-presented. In log–log plots renormalization by multiplication is a simple translation of the axes and may be reported by marking a single datum point on the original plot and carrying it through to the normalized presentation.

A second variable that can be particularly useful is temperature. It is, of course, essential that all measurements should be carried out at constant temperatures. If the temperature changes during a measurement run then significant errors will be introduced. Generally the effect of temperature is most significant in the magnitude of the relaxation time τ and a commonly observed form for the relaxation time is

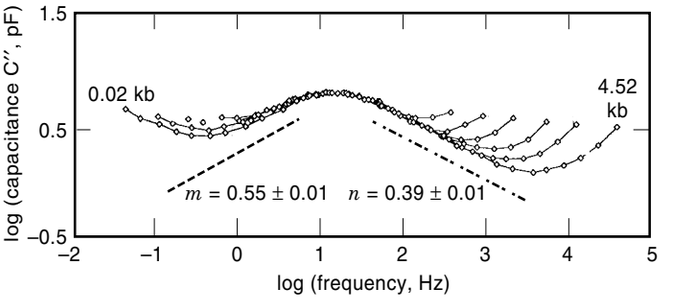

Figure 13. Normalization of the data for polythene under pressure, Fig. 6(a). The normalization has been carried out in terms of the pressure and shows that the *form* of the loss dispersion does not change with the pressure. The data can be fitted with a function having $m = 0.55 \pm 0.02$ and $n = 0.39 \pm 0.02$.

$$\tau = \tau_0 \exp(-\varphi/kT) \tag{49}$$

the characteristic of a thermally activated or Arrhenius behavior with φ the activation energy in electron volts when k, Boltzmann's constant, is taken as $0.86\ 10^{-4}$ eV/K and the temperature is in degrees kelvin. As a guide 1 eV gives approximately 300% change in τ for each 10°C change of temperature in the region of room temperature, and this energy is the order of magnitude of local binding energies in polymeric materials.

This argument can be used in a different framework. Assume that we are considering a dielectric response spectrum which contains more than one dispersion process. Only if the temperature dependencies of the individual dispersions are identical will we be able to superimpose the individual processes. Hence we can use the superposition technique to determine, and characterize, the number of independent processes of relaxation.

INTERFACIAL POLARIZATION

At an interface between two dielectric materials of different permittivities there will be a layer of surface charge. Consider a simple plane interface with the materials of permittivities ϵ_1 and ϵ_2 and a voltage V applied. We consider that the capacitors are of the same area A and that the permittivities and thicknesses are ϵ_1 and d_1 and ϵ_2 and d_2, respectively. At the boundary between the insulators the voltage is continuous, but when ϵ_1 is not equal to ϵ_2, the electric fields in the two media are of different magnitude. The discontinuity in permittivity results in a surface layer of charge at the interface. Consider, as a model system, two capacitors mounted in series, for which we have

$$C_0^{-1} = C_1^{-1} + C_2^{-1}$$

in which $C_1 = \epsilon_0\epsilon_1 A/d_1$ is the first capacitor over which the ac voltage drop is V_1 and V is the total voltage applied. Substi-

tuting for the individual capacitances and dividing by the common terms A and ϵ_0 gives

$$E_0 = E_1\epsilon_1\frac{d_1}{d_1+d_2} + E_2\epsilon_2\frac{d_2}{d_1+d_2} \tag{50}$$

where E_0 is the applied voltage, V, divided by the total thickness, $d_1 + d_2$. When ϵ_1 is not equal to ϵ_2 there will be a charge layer at the internal interface. The charge at the surfaces of the individual capacitors are $\pm\sigma_1$ and $\pm\sigma_2$, where $\sigma_1 = E_1\epsilon_1$ and $\sigma_2 = E_2\epsilon_2$ and this gives the total charge at the internal interface as

$$\sigma_i = \sigma_1 - \sigma_2 = E_1\epsilon_1 - E_2\epsilon_2 \tag{51}$$

which will be zero when $\epsilon 1 = \epsilon 2$, that is, when the interface lies between two pieces of the same material. In the general case when the interface is between two dissimilar materials the interface charge forms an additional component of the dielectric response, the magnitude of which is linearly dependent on the magnitude of the voltage applied across the layered sample and the interface acts as an additional polarization process.

In a material containing many interfaces, such as a random array of regular or irregular particles embedded in a host of different permittivity, each particle will act, on a molecular scale, as a large polarizable entity and contribute to the total polarization. From such a model Wagner (26) proposed the function

$$\frac{\epsilon-\epsilon_2}{\epsilon+2\epsilon_2} = \frac{\epsilon_1=\epsilon_2}{\epsilon_1+2\epsilon_2}\,\theta \tag{52}$$

to describe the permittivity ϵ of the inhomogeneous material for which θ is the volume fraction of particles of permittivity ϵ_2 embedded in the medium of permittivity ϵ_1. This function and other similar formulas are considered by Clausse (27) in his review of particulate systems, but no simple and effective dispersion function has yet been found that is applicable to the general case for which the particles have a distribution of sizes and dielectric properties.

Barrier Layers

One particular case of interfacial polarization is of interest and can be analyzed in detail. The range of relative permittivities in insulating materials is limited from about 2 to about 100, unless we are working with high-quality ferroelectrics for which the permittivity can be significantly higher. Hence we would normally expect dispersion magnitudes for a mixed system to lie somewhere in this range. Occasionally in experimental work on solids and liquids and particularly at low, that is, submegahertz, frequencies anomalously large values for the permittivity are observed, of the order of thousands or greater. In these cases there is cause to consider what is happening in the measurement cell, particularly at one or both of the electrodes. At these low frequencies the simple cell, using two conducting electrodes and with the sample mounted between them in a planar or concentric geometry, is sufficient and we can write the capacitance of the system is $\epsilon_r\epsilon_0\xi$, where ξ is a geometrical factor with dimensions of length and for the plane-parallel system is given by the area of the electrodes divided by the spacing between the parallel plates. However, if the electrodes make a poor contact with the sample there is a second capacitance in series with that due to the bulk material. The imperfect contacts have not only resistive but capacitive properties and can be considered as a pair of capacitors electrically in series with the sample but with a combined thickness, d_b, which will be much less than that of the sample and hence a barrier capacitance $C_b(\omega)$ which will be much greater than the sample capacitance $C(\omega)$. For capacitors connected electrically in series one inverts the sum of the impedances for each of the components to obtain the admittance and hence, after division by ω, the capacitance. Following this procedure we have

$$\frac{1}{C(\omega)} = \frac{1}{C_s - iG_s/\omega} + \frac{1}{C_b(\omega)} \tag{53}$$

$$C(\omega) = \frac{C_b(\omega)(C_s - iG_s/\omega)}{C_b(\omega) + C_s - iG_s/\omega}$$

$$\simeq C_b \qquad when\ G/\omega \gg C_b \gg C_s \tag{54a}$$

$$\simeq C_s - iG/\omega \qquad when\ C_b \gg G_s/\omega \gg C_s \tag{54b}$$

where the sample conductance, G_S, allows charging of the barrier capacitance and at sufficiently low frequencies, $\omega \leq (C_bG_s)^{-1}$, the observed capacitance is due entirely to the barrier layers. When the frequency is high, ac coupling through the barriers makes their impedance low and the bulk properties are recovered.

When measuring solutions containing free ions the bulk conductance will be high and when the discharge of the ions at the electrodes is inefficient this results in the formation of thin barrier layers of low conductance, and high capacitance, at the surfaces of the electrodes. Using conducting solutions and noninteractive metal electrodes such as platinum, it is possible to measure the thickness of the charge barrier layer buildup at the electrode as a function of a dc bias voltage on top of the small-magnitude ac measuring voltage. This technique has been developed into cyclic voltammetry and is used extensively by surface layer chemists.

An example of a clear barrier effect has been observed by Taylor and MacDonald (28). The observations were made with a cell containing a solution of potassium chloride in water and used copper electrodes. The data indicate the buildup of a partial blocking surface layer at the electrodes, probably

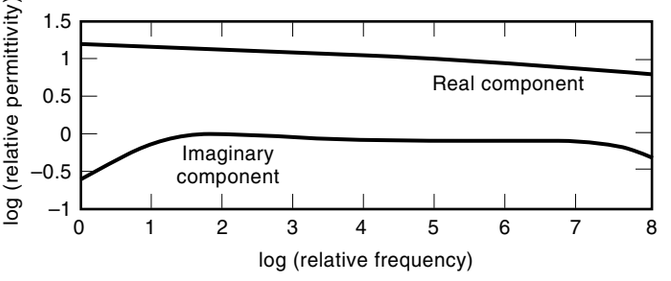

Figure 14. An example of a limited-range, frequency-independent loss. As described in the text a suitable summation of two dispersion processes can lead to a weak dispersion in the loss. However, it is not possible to obtain a loss that is perfectly independent of the frequency for this would result in the loss having zero magnitude. The parametric values for the two DH dispersions were $m_1 = 0.8$, $n_1 = 0.9$ $\tau_1^{-1} = 10$, $\chi_1 = 7$, $m_2 = 0.1$, $n_2 = 0.4$, $\tau^{-1}2 = 3 \times 10^7$, $\chi_2 = 5$, and $\chi_\infty = 5$.

of copper chloride, which acts as a barrier to further charge exchange. The barrier layer conducts charge, but at a lower rate than the solution. At the highest frequencies the response is that of the salt solution conductance in parallel with the capacitance of the liquid filled cell. As the frequency decreases to a few hertz, the solution's conductance is truncated by the initial electrode barrier layer, which has a large capacitance, and, hence, we are led to the conclusion that the thickness of the barrier layer is less than two orders of magnitude smaller than the cell plate spacing. At the lowest frequencies we do not observe the classic simple quasi-dc frequency response expected for a weak conduction through the barrier but a continual increase in the frequency exponent as the frequency is decreased.

Many of the materials that are in common use are inhomogeneous in the sense that either the structures are not perfectly crystalline and are formed either as crystallites or large polymeric molecules embedded in an unstructured matrix or are formed as stacked layers during their manufacturing process. When the particles or sheets are electrically active and can be polarized, dielectric spectroscopy is an effective and growing technique for the assessment of the nature and reproducibility of the structures.

Frequency-Independent Loss

When dielectrics are used for insulation of power cables the imaginary component of the permittivity is in phase with the applied voltage and generates a power loss in the form of heat. It is usual for these cables to run above the ambient temperature but an excessive amount of power loss is unacceptable. Furthermore, particularly for communication work, there is an advantage in having a frequency-independent loss characteristic in order that the signal should not be distorted during transmission. Obviously, working in the region of frequency for which there is a maximum in the loss would be undesireable. We characterize a dispersive process by considering a fractional power law of exponent $1 - n$. With $n = 0$ we would obtain the ideal situation with no dispersion in the real permittivity, but this appears to be unattainable in practice.

The second choice is to have a nondispersive, "flat," loss response over the frequency range that is of interest (29). In order to understand the difficulties implicit in obtaining this form of response we start by defining two frequencies ω_l and ω_h as the lowest and highest frequencies that we take to define the range over which we wish the loss to be constant and consider a frequency ω within this range. Taking the inverse Kramers–Kronig transform of the constant loss χ''_c, which is a Hilbert transform (28) we obtain (30)

$$\chi'(\omega) = \chi_0 \log\left(\frac{\omega_h - \omega}{\omega - \omega_l}\right) \tag{55}$$

and for $\chi''(\omega)$ to be close to its maximum value, and hence the loss small, we wish the operating frequency to be close to the lower frequency for the constant loss band. However, because of the presence of this loss component the real component is required to be dispersive and more strongly dispersive at the lower frequencies, which negates our requirements unless the magnitude of the higher-frequency dispersive processes, ϵ_∞, is large compared to the magnitude of the loss component.

Having shown that no single dispersion process is suitable we have to consider the third alternative, which is that more than one loss process is operative and that the lower wing of the upper-frequency process overlaps, in frequency, the high-frequency dispersion of the lower rate process. In this case there will exist a frequency for which the loss has zero gradient and that will lie somewhere between the loss peak values. If the loss processes are both broad, that is, in the nomenclature of Fig. 8, m is to be small for the higher-frequency process and n approaches unity for the lower-frequency process, then the region of "flat" loss may cover a reasonable range. However, both processes add to the dispersion in $\epsilon'(\omega)$ and, once again, the capacitance cannot be constant.

We show in Fig. 13 the overlapping of two dispersions that results in an almost nondispersive loss but, both practically and fundamentally, there can never be a constant loss over any finite region of frequency, for this requires that

$$\chi''_1(\omega\tau_1)^{-b} + \chi''_2(\omega\tau_2)^a = \text{const} \tag{56}$$

in the range $\tau_1^{-1} > \omega > \tau_2^{-1}$. The figure shows that the nearest approach to this is when both a and b are close to zero, that is, m is small and n approaches unity, so that we are considering very broad loss peaks, the relevant loss gradients in the midfrequency region are of the order of one tenth, which will, as a consequence, be expected to be of small magnitude.

We conclude that as the real components of the susceptibility are finite and of constant magnitude, at frequencies well below the relevant relaxation frequency, and the equivalent loss components are decreasing in this region, there is an essential difference between the components of the loss angle and hence in the fraction of energy lost in the dielectric. It is absolute that a perfectly frequency-independent loss gives a dispersion in the real permittivity and that a frequency-independent permittivity necessitates that there should be no equivalent loss. These conditions are a trivialization of the fundamental nature of the Kramers–Kronig transform and cannot be circumvented. The commonly observed parallelism of the fractional exponent power law in the susceptibilities requires that a constant capacitance can only be obtained when there is zero loss. A finite loss will always lead to a dispersion in the capacitive component. A minimization of the loss dispersion can be achieved, but to do so requires the presence of higher-frequency dispersion processes of significant magnitude.

CONCLUSIONS

Much of the literature on the dielectric properties of materials has reported the polarizability of particular chemical compounds either in solutions or in solids, or in electrically inert matrices or as crystals. For chemistry-based investigators the peculiar advantage of these measurements are the labeling of particular atomic configurations through the magnitude of the observed polarizabilities. An opposing stance is taken by electrical engineers, who are seeking materials that ideally have no ac loss and high permittivities for energy storage, or zero loss and a low admittance for the insulation of power cables. In the latter case the permittivity at power frequencies would be a significant observation as the real component is a measure of all the loss processes at higher frequencies,

via the Kramers–Kronig transform, and the loss a direct measure of the quality of the cable when in use. However, it is as a diagnostic tool for gaining information about individual loss processes that dielectric spectroscopy has a significant role to play in the material science of insulators and dielectrics while the recent developments in measuring equipment has resulted in an improved accessibility to quality data.

It has been accepted that the classic Debye dispersion is not observed in the majority of the materials that are of interest to electrical engineers. There is a growing body of information that the variation from the classic Debye behavior is based on the dissipation of the polarization on two time scales, separated by a Debye-like relaxation time. For times shorter than this, that is, for frequencies in excess of the relaxation frequency, the change in polarization must be constrained to the locality of the polarizing entity. Conversely, at long times, low frequencies, equilibrium will be approached within a cycle by the dissipation of energy over an extended sphere of influence. From this simple cooperative model it is possible to propose that the independent exponents that are observed at high and low frequencies relate to different couplings or exchanges in the matrix within which the active, driving, dipole exists. In developing our understanding of the significance of the lack of Debye quality of the observed relaxation behavior we are able to support the use of dielectric spectroscopy as an effective tool from which can be obtained quantitative information regarding the interaction of a dipole and the micro and macro systems in which it exists.

In order to carry out this development it is necessary to review the earlier work in the field, much of which is of good quality, and use the information gleaned from this overview in order to guide future development. It is clear that the fractional power-law behavior, which has long been established, experimentally indicates fractal exchange processes for the disipation of energy. In this model the low-frequency parameter is a measure of the efficiency of exchange at long times and the high-frequency parameter an equivalent measure for short times, with respect to the characteristic relaxation time. We note, in this context, that elsewhere in the present volume both ferroelectric and piezoelectric materials are reported. The former as a group have close to Debye relaxation behavior and, like water, possess highly ordered structures at both short and long ranges.

Our understanding of dielectrics has not greatly advanced since the intensive effort that led to the widespread use of electricity as the convenient power source in the early part of the century. Recent improvements in equipment have developed broad-frequency-band measuring facilities and the possibility of observing charge, and electric field, distributions in insulators that are under voltage stress. The latter technique, in particular, is giving data that are challenging the fundamental concepts that we have been applying for over a century and cannot do other than lead to a new understanding of the nature of charge flow and storage in weak conductors which will, in turn, lead to significant and effective developments.

BIBLIOGRAPHY

1. M. Faraday, Experimental research in electricity, *Phil. Trans.* **79**: 1–12, 1839.
2. R. Clausius, *Die Mechanische Wärmetheorie,* Braunschweig, 1879, p. 62.
3. O. F. Mossotti, *Bibl. Univ. Modena,* **6**: 193, 1847.
4. R. Kubo, Statistical-mechanical theory of irreversible processes I, *J. Phys. Soc. Jpn.,* **12**: 570–586, 1957.
5. C. Brot, *Dielectric and Other Related Molecular Processes,* Vol. 2, London: The Chemical Society, 1973, pp. 1–47.
6. R. Kronig, On the theory of dispersion in x-rays, *J. Opt. Soc. Am.,* **12**: 547–557, 1926.
7. R. Kronig and H. A. Kramers, Absorption and dispersion in X-ray spectra, *Zeitschrift fur Physik,* **48**: 174–179, 1928.
8. I. S. Gradshteyn and I. M. Ryzhik, *Tables of Integrals, Series, and Products,* New York: Academic Press, 1980, Function 3.241.3.
9. P. Debye, Results of kinetic theory of dielectrics, *Phys. Zeitschrift,* **13**: 97–100, 1912.
10. K. S. Cole and R. H. Cole, Dispersion and absorption in dielectrics, *J. of Chem. Phys.,* Vol. 9, pp. 341–351, 1941.
11. J. M. Alison, A dielectric study of lossy materials over the frequency range 4 to 82 GHz, Ph.D. Thesis, University of London, 1990.
12. M. G. M. Richards, The development of a technique to measure the complex conductivity of liquids and biological tissue at 90 GHz, Ph.D. Thesis, University of London, 1993.
13. J. M. Alison and R. J. Sheppard, Dielectric properties of human blood at microwave frequencies, *Phys. Med. Biol.,* **38**: 971–978, 1993.
14. R. M. Hill, Characterization of dielectric materials, *J. Mater. Sci.,* **16**: 118–124, 1981.
15. D. W. Davidson and R. H. Cole, Dielectric relaxation in glycerine, *J. Chem. Phys.,* **18**: 1417, 1950.
16. J. A. Sayre, S. R. Swanson, and R. Boyd, The effect of pressure on the volume and dielectric relaxation of linear polyethylene, *J. Polym. Sci.: Polym. Phys. Ed.,* **16**: 1739–1759, 1978.
17. G. E. Johnson, E. W. Andrews, and T. Firukama, Fourier transform dielectric spectroscopy utilizing a real time executive (RTE) system, *IEEE Proc. CEIDP,* 250–263, 1981.
18. S. Havriliak and S. Negami, A complex analysis of the α-dispersion in some polymer systems. *Polym. Sci.,* **C14**: 99, 1966; A complex plane representation of dielectric and mechanical relaxation processes, *Polymer,* **8**: 161–210, 1967.
19. A. K. Jonscher, A new model of dielectric loss in polymers, *Colloid and Polym. Sci.,* **253**: 231–250, 1975.
20. L. A. Dissado and R. M. Hill, A cluster approach to the structure of imperfect materials and their relaxation spectroscopy, *Proc. R. Soc. London,* **A 390**: 131–180, 1983.
21. R. Kohlrausch, *Ann. Phys. (Leipzig),* **12**: 393, 1847.
22. G. Williams and D. C. Watts, Non-symmetrical dielectric relaxation behaviour arising from a simple empirical decay function, *Trans. Faraday. Soc.,* **66**: 80–85, 1970.
23. C. J. F. Böttcher and P. Bordewijk, *Theory of Electric Polarization,* Amsterdam: Elsevier Press, 1973, vol 2, App. 5, Sec. 6, pp. 523–524.
24. H. Pellat, Polarization of dielectrics, *Annal. Chim. Phys.,* **18**: 150–181, 1899.
25. G. Giraud, J. Clerk, and J. M. Laugier, Dielectric behaviour of a composite medium: A percolation model, *Proc. 1st. ICSD Conf.,* 1983, pp. 139–142.
26. K. Wagner, Dielectric properties of various insulating materials, *Arch. Elektrotek.,* **3**: pp. 67–106, 1914.
27. M. Clausse, in P. Becker (ed.), *Encyclopedia of Emulsion Technology,* New York: Marcel Dekker, 1983, vol. 1.

28. M. Taylor and A. G. McDonald, AC admittance of the metal/insulator/electrolyte interface, *J. Phys. D: Appl. Phys.,* **20**: 1277–1283, 1987.
29. A. K. Jonscher, *Universal Relaxation Law,* New York: Chelsea Dielectrics Press, 1996, p. 165 et. seq.
30. A. Erdélyi (ed.), Tables of Integral Transforms, Transform 15.2, New York: McGraw-Hill, 1954.
31. R. M. Fuoss and J. G. Kirkwood, Electrical properties of solids VIII, *J. Amer. Chem. Soc.,* **63**: 385–394, 1941.
32. L. A. Dissado and R. M. Hill, Quasi-DC conduction, *Faraday Trans. 2, The Chem. Soc.,* **80**: 291–319, 1984.

Reading List

C J. F. Böttcher and P. Bordeqijk, *Theory of Electric Polarization,* Vols. 1 and 2, Amsterdam: Elsevier, 1978.
A. K. Jonscher, *Dielectric Relaxation in Solids,* London: Chelsea Dielectrics Press, 1983.
H. G. McCrum, B. E. Read, and G. Williams, *Anelastic and Dielectric Effects in Polymeric Solids,* New York: Dover, 1967.
B. K. P. Scaife, *Principles of Dielectrics,* Oxford: Clarendon, 1989.

R. M. HILL
J. M. ALISON
King's College London

DIELECTRIC PROPERTIES. See PASSIVATION.

DIELECTRIC RELAXATION. See LOSS-ANGLE MEASUREMENT.